



OPEN ACCESS

EDITED BY

Xiao Chang,
Children's Hospital of Philadelphia,
United States

REVIEWED BY

Cen Wu,
Kansas State University, United States
Deli Mao,
The Seventh Affiliated Hospital of Sun
Yat-sen University, China

*CORRESPONDENCE

Guo-Liang Shen,
sdfyysgl@163.com

[†]These authors have contributed equally
to this work

SPECIALTY SECTION

This article was submitted to
Computational Genomics,
a section of the journal
Frontiers in Genetics

RECEIVED 18 November 2021

ACCEPTED 04 July 2022

PUBLISHED 22 July 2022

CITATION

Huang C-H, Han W, Wu Y-Z and
Shen G-L (2022), Identification of
aberrantly methylated differentially
expressed genes and pro-tumorigenic
role of KIF2C in melanoma.
Front. Genet. 13:817656.
doi: 10.3389/fgene.2022.817656

COPYRIGHT

© 2022 Huang, Han, Wu and Shen. This
is an open-access article distributed
under the terms of the [Creative
Commons Attribution License \(CC BY\)](#).
The use, distribution or reproduction in
other forums is permitted, provided the
original author(s) and the copyright
owner(s) are credited and that the
original publication in this journal is
cited, in accordance with accepted
academic practice. No use, distribution
or reproduction is permitted which does
not comply with these terms.

Identification of aberrantly methylated differentially expressed genes and pro-tumorigenic role of KIF2C in melanoma

Chun-Hui Huang^{1,2†}, Wei Han^{3†}, Yi-Zhu Wu^{1,2†} and
Guo-Liang Shen^{1,2*}

¹Department of Burn and Plastic Surgery, The First Affiliated Hospital of Soochow University, Suzhou, China, ²Department of Surgery, Soochow University, Suzhou, China, ³Institute of Regenerative Biology and Medicine, Helmholtz Zentrum München, Munich, Germany

Background: Skin Cutaneous Melanoma (SKCM) is known as an aggressive malignant cancer, which could be directly derived from melanocytic nevi. However, the molecular mechanisms underlying the malignant transformation of melanocytes and melanoma tumor progression still remain unclear. Increasing research showed significant roles of epigenetic modifications, especially DNA methylation, in melanoma. This study focused on the identification and analysis of methylation-regulated differentially expressed genes (MeDEGs) between melanocytic nevus and malignant melanoma in genome-wide profiles.

Methods: The gene expression profiling datasets (GSE3189 and GSE114445) and gene methylation profiling datasets (GSE86355 and GSE120878) were downloaded from the Gene Expression Omnibus (GEO) database. Differentially expressed genes (DEGs) and differentially methylated genes (DMGs) were identified via GEO2R. MeDEGs were obtained by integrating the DEGs and DMGs. Then, a functional enrichment analysis of MeDEGs was performed. STRING and Cytoscape were used to describe the protein-protein interaction (PPI) network. Furthermore, survival analysis was implemented to select the prognostic hub genes. Next, we conducted gene set enrichment analysis (GSEA) of hub genes. To validate, SKCM cell culture and lentivirus infection was performed to reveal the expression and behavior pattern of KIF2C. Patients and specimens were collected and then immunohistochemistry (IHC) staining was conducted.

Abbreviations: SKCM, skin cutaneous melanoma; DEGs, differentially expressed genes; DMGs, differentially methylated genes; MeDEGs, methylation-regulated differentially expressed genes; DAVID, the Database for Annotation, Visualization and Integrated Discovery; GEPIA, Gene Expression Profiling Interactive Analysis; GO, gene ontology; BP, biological process; CC, cellular component; MF, molecular function; KEGG, Kyoto Encyclopedia of Genes and Genomes; PPI, protein-protein interaction; TCGA, the Cancer Genome Atlas; GTEx, Genotype-Tissue Expression project; OS, overall survival; GSEA, gene set enrichment analysis; MARK, mitogen-activated protein kinase.

Results: We identified 237 hypomethylated, upregulated genes and 182 hypermethylated, downregulated genes. Hypomethylation-upregulated genes were enriched in biological processes of the oxidation-reduction process, cell proliferation, cell division, phosphorylation, extracellular matrix disassembly and protein sumoylation. Pathway enrichment showed selenocompound metabolism, small cell lung cancer and lysosome. Hypermethylation-downregulated genes were enriched in biological processes of positive regulation of transcription from RNA polymerase II promoter, cell adhesion, cell proliferation, positive regulation of transcription, DNA-templated and angiogenesis. The most significantly enriched pathways involved the transcriptional misregulation in cancer, circadian rhythm, tight junction, protein digestion and absorption and Hippo signaling pathway. After PPI establishment and survival analysis, seven prognostic hub genes were CKS2, DTL, KIF2C, KPNA2, MYBL2, TPX2, and FBL. Moreover, the most involved hallmarks obtained by GSEA were E2F targets, G2M checkpoint and mitotic spindle. Importantly, among the 7 hub genes, we found that down-regulated level of KIF2C expression significantly inhibited the proliferative ability of SKCM cells and suppressed the metastasis capacity of SKCM cells.

Conclusions: Our study identified potential aberrantly methylated-differentially expressed genes participating in the process of malignant transformation from nevus to melanoma tissues based on comprehensive genomic profiles. Transcription profiles of CKS2, DTL, KIF2C, KPNA2, MYBL2, TPX2, and FBL provided clues of aberrantly methylation-based biomarkers, which might improve the development of precision medicine. KIF2C plays a pro-tumorigenic role and potentially inhibited the proliferative ability in SKCM.

KEYWORDS

melanoma, methylation, hub genes, prognosis, nevus, KIF2C

Background

Skin cutaneous melanoma (SKCM) is an aggressive tumor that is the fifth and sixth most common malignant tumor in men and women respectively (Siegel et al., 2020). Each year, melanoma accounts for over 80% of skin cancer-related deaths in the world (Schadendorf van Akkooi et al., 2018). According to the Clark model, the pathogenesis of melanoma assumes that numerous steps are required for the progression from melanocytes to malignant melanoma, including the formation of banal nevi, dysplastic nevi, melanoma *in situ*, and invasive melanoma (Wallace et al., 1984). However, the molecular mechanisms underlying the malignant transformation of melanocytes and melanoma tumor progression still remain unclear. Nowadays, as for the primary tumors, surgical resection is usually preferred, while metastatic melanoma is much more difficult to treat with radiotherapy and chemotherapy, which means that early diagnosis is essential (Gadeliya Goodson and Grossman, 2009). Recently developed immunotherapies and targeted therapies show promise for improving the prognosis of patients with advanced melanoma (Flaherty et al., 2012). Identification of melanoma-associated oncogenes informs

different therapeutic strategies, and small molecule inhibitors are available to target specific proteins involved in the pathogenesis of melanoma (Mohammadpour et al., 2019). Unfortunately, most patients with melanoma, which are initially diagnosed with highly aggressive and progressive disease, are not candidates for curative therapies (Schadendorf van Akkooi et al., 2018).

DNA methylation is known as a central epigenetic modification, and a significant regulator of gene expression, which can inhibit the binding of transcription factors or the recruitment of repression proteins (Moore et al., 2013). Aberrant promoter methylation of genes that control cell cycle and apoptosis can contribute to the disruption of normal cell division and carcinogenesis (Schinke et al., 2010). Importantly, aberrant DNA methylation is regarded as an epigenetic hallmark of melanoma and plays a significant part in the formation as well as progression of melanoma (Schinke et al., 2010; Goran Micevic et al., 2017). Methylation of CpG islands appears early in tumorigenesis and the epigenetic changes can be identified in serum, sputum, and urine samples which means it might contribute to the development of molecular strategies for cancer detection as well as function as a biomarker of cancer

recurrence after excision (James and Herman, 2003). Furthermore, it was reported that hypermethylation correlated with worse prognosis as well as drug resistance (Mori et al., 2005). Increasing evidence showed a vital role for both global hypomethylation of oncogenes and hypermethylation of tumor suppressor genes in tumor development and progression, including in melanoma. For example, methylation silencing of PTEN, an inhibitor of PI3K signaling, was closely related to a worse prognosis in melanoma patients (Lahtz et al., 2010). In addition, the hypermethylation of WIF1, TFPI2, RASSF1A, and SOCS1 has been considered as significant participants in the melanoma initiation and progression (Tanemura et al., 2009). Although research on the identification of separate genes with specific hypermethylation or hypomethylation in SKCM are available, comprehensive network studies based on gene expression, methylation profiles and associated pathways have been greatly insufficient.

Over the last decade, bioinformatics technology has emerged as an indispensable tool for tumor research. It mainly focuses on genomics and proteomics to identify genotypes and phenotypes associated with immune infiltration, tumorigenesis and progression of melanoma to guide the development of targeted therapy (Fan et al., 2018; Zhang et al., 2019). For example, Weiyang Cai et al. (2018) identified many differentially methylated genes (DMGs) related to lymph node metastasis in melanoma and were closely associated with the prognosis of melanoma patients. Duan et al. (2018) found three methylated genes (*ARX*, *DDB2*, and *MBP*) that may be closely associated with the underlying mechanism in melanoma progression. Although methylation changes in SKCM were studied in many research, countless issues are still unclear.

Here, we performed an integrated bioinformatics analysis based on gene expression profiling by high-throughput sequencing (GSE3189 and GSE114445) and gene methylation profiling microarray (GSE86355 and GSE120878). The methylation-regulated differentially expressed genes (MeDEGs) were screened and performed functional enrichment analysis. Furthermore, protein-protein interaction (PPI) networks and survival analysis were used to identify new prognostic biomarkers and therapeutic targets for future research in melanoma.

Methods

Acquisition and standardization of raw microarray dataset

We downloaded the gene expression profiling datasets generated by high-throughput sequencing (GSE3189 and GSE114445) and the microarray-based gene methylation profiling datasets (GSE120878 and GSE86355) from the Gene Expression Omnibus database (GEO, <https://www.ncbi.nlm.nih.gov/geo/>). Totally 18 nevi and 45 melanoma samples were included in GSE3189 (platform:

GPL96 Affymetrix Human Genome U133A Array) while 5 nevi and 16 melanoma samples were enrolled in GSE114445 (platform: GPL570 Affymetrix Human Genome U133 Plus 2.0 Array). As for the DNA methylation datasets, GSE120878 included a total of 73 nevi and 89 primary SKCM tissues, while GSE86355 included altogether 14 nevi and 33 primary SKCM tissues. Both of these two methylation microarrays were based on the GPL13534 platform (Illumina HumanMethylation450 BeadChip).

Identification of methylation-regulated differentially expressed genes

GEO2R (<http://www.ncbi.nlm.nih.gov/geo/geo2r/>) is a web tool to make a comparison of two or more groups of samples in a GEO Series to screen genes that are differentially expressed across specific experimental conditions. In the present study, GEO2R was used to identify the differentially expressed genes (DEGs) as well as the differentially methylated genes (DMGs). $|t| > 2$ and $p < 0.05$ were considered statistically significant. Then, hypomethylation-high expression genes were obtained after the overlap of upregulated and hypomethylated genes, and hypermethylation-low expression genes were obtained after the overlap of downregulated and hypermethylated genes. The hypomethylation-high expression genes and hypermethylation-low expression genes were identified as methylation-regulated differentially expressed genes (MeDEGs).

Functional enrichment analysis

The Database for Annotation, Visualization and Integrated Discovery (DAVID, <https://david.ncifcrf.gov/>) is a straightforward web tool that can provide integrative and systematic annotation for users to unravel biological interactions of multiple genes. It was utilized to perform functional and pathway enrichment analyses. Gene ontology (GO) analysis including the biological process (BP), cellular component (CC), molecular function (MF) and Kyoto Encyclopedia of Genes and Genomes (KEGG) pathway enrichment analysis were conducted for the selected MeDEGs by DAVID (Ashburner et al., 2000; Huang et al., 2007). p -value < 0.05 was considered statistically significant.

Protein-protein interaction network construction and identification of hub genes

In this study, STRING (<http://string-db.org/>; version 11.0) was adopted to describe protein co-regulation of hypomethylation-high expression genes and

hypermethylation-low expression genes respectively and measure functional interactions among nodes (Franceschini et al., 2013). The interaction specificity score >0.4 (the default threshold in the STRING database) was considered statistically significant. Cytoscape (version 3.6.0) was used to visualize interaction networks obtained from STRING (Smoot et al., 2011). MCODE (version 1.4.2) of Cytoscape is a plug-in to cluster a given network to identify densely connected regions based on topology (Bandettini et al., 2012). It was utilized to find the most related module network with selection threshold as follows: MCODE scores >5 , degree cutoff=2, node score cut-off=0.2, Max depth=100 and k-score=2.

Survival analysis

Gene Expression Profiling Interactive Analysis (GEPIA, <http://gepia.cancer-pku.cn/>) is an online tool that can provide customizable functionalities based on data from The Cancer Genome Atlas (TCGA; <https://tcga-data.nci.nih.gov/tcga/>) and the Genotype-Tissue Expression project (GTEx; <https://www.gtexportal.org/home/index.html>) (Tang et al., 2017). GEPIA performs survival analysis based on gene expression levels, using a log-rank test for the hypothesis evaluation. The horizontal axis (x-axis) represented the time in days, and the vertical axis (y-axis) showed the probability of surviving or the proportion of people surviving. The lines presented the survival curves of two groups.

Validation of hub genes

Oncomine (<https://www.oncomine.org>) is an online database that allows users to collect, normalize, and analyze gene expression profiling data for tumor samples (Rhodes et al., 2007). Oncomine database was utilized to validate the differential expression of hub genes between SKCM and nevus samples. After choosing the catalog of SKCM and nevus tissue, a comparison of mRNA expression levels was made. The cBioPortal (<http://cbioportal.org>) is an open-access resource for users to search for multidimensional cancer genomics datasets which provide access to data for over 5000 tumor samples from 20 cancer studies (Cerami et al., 2012). We used cBioPortal to investigate the genetic alterations of hub genes as well as the correlation between methylation status and gene expression.

Transcription factor network and data processing of gene set enrichment analysis

Transcription factor regulation networks of hub genes were constructed by using R software (Version 3.3.2). Significant nodes involved in co-regulation of *CKS2*, *DTL*, *KIF2C*,

KPNA2, *MYBL2*, *TPX2* and *FBL* were described in circle plots (including transcription factor regulation-DNA binding, related lncRNA, targeted miRNA and protein-protein interaction). Based on data from the TCGA database, GSEA tool (version 2.10.1 package) was used to predict associated up- and down-regulated genes and their significantly involved hallmarks pathways (Subramanian et al., 2005). Student's t-test statistical score was implemented in consistent pathways and the mean of the differentially expressed genes was calculated for each analysis. A permutation test with 1000 times was utilized to recognize the greatly involved pathways. The adj. P using Benjamini and Hochberg (BH) and false discovery rate (FDR) method by default were used to correct for the occurrence of false-positive results. Significantly related genes were defined with an adj. $p < 0.01$ and $FDR < 0.25$.

Cell culture and lentivirus infection

The human SKCM cell lines (A375) are widely used and representative in various SKCM studies, which were obtained from the Cell Bank of Shanghai Institutes of Biological Sciences, Chinese Academy of Sciences (Shanghai, China). The SKCM cells were cultured in RPMI 1640 medium (Gibco, CA, United States) with 10% fetal bovine serum (Gibco, United States) and 1% penicillin-streptomycin solution (Gibco, CA, United States) at 37°C in a humidified incubator containing 5% CO₂. The medium was refreshed every 2 days. To establish a stable cell line and intervene the expression of *KIF2C*, lentiviral vectors and small interfering RNA (siRNA; siRNA-1: 5'-GCCCACTGAATAAGCAAGAAT-3'; siRNA-2: 5'-GCCCGAATGATTAAGAATTT-3') targeting *KIF2C* (NM_006845) were obtained from GeneChem (Shanghai, China). Cells were transfected and underwent sterility testing with lentivirus, strictly following the manufacturer's instructions (GeneChem, China).

Quantitative reverse transcriptase-polymerase chain reaction

We used TRIzol reagent (Solarbio, China) to extract total RNA from A375 cells, and transcribed them into complementary DNA. Subsequently, SYBR green PCR Master Kit (QIAGEN, Germany) was used for qRT-PCR. The primer sequences for *KIF2C* and β -actin were designed and displayed in Supplementary Table S1. The reaction conditions of qRT-PCR were conducted according to manufacturers' protocols (Livak and Schmittgen, 2001) and briefly shown as follows: initial heat activation at 95°C for 2 min and denaturation at 95°C for 5 s, consecutively followed by 40 cycles of 60°C for 30 s and a final extension step. The level of RNA expression was determined by the original Ct value and the $2^{-\Delta\Delta Ct}$ method.

Patients and specimens collection

All procedures performed in this study involving human participants were in accordance with the Declaration of Helsinki. The study was approved by the ethics committee of the First Affiliated Hospital of Soochow University and informed consent was taken from all the patients. We collected fresh samples from 33 patients at the First Affiliated Hospital of Soochow University from 2019 to 2021. All patients underwent surgeries, had not received preoperative therapy, and were pathologically diagnosed with SKCM. Tissue specimens were obtained during surgery and immediately preserved at -80°C .

Immunohistochemistry staining

We collected 33 SKCM tissues from patients undergoing surgery at the First Affiliated Hospital of Soochow University. All of the tissues were pathologically confirmed to be SKCM and fixed in 4% paraformaldehyde overnight and embedded in paraffin. Sections were deparaffinized with xylene and hydrated with graded alcohols. Subsequently, the sections were incubated with 3% H_2O_2 for 10 min at 37°C and washed in phosphate-buffered saline (PBS). The sections were then incubated with 50 μl of rabbit monoclonal anti-KIF2C antibody (No. ab71706, Abcam, United States) at 4°C overnight. The dilution ratio of the antibody was dependent on the recommended dilution ratio in the specifications. Next, the sections were incubated with PV-6001 (ZSBG, Beijing, China) for 30 min at 25°C . Finally, we stained the slices with 3,3'-diaminobenzidine and hematoxylin for detection. A positive reaction was defined as cytoplasm showing a brown signal. The degree of immunostaining was performed independently by 2 experienced pathologists. The immunostaining score depended on the percentage of positive cells (range: 0–4%; 0, <5%; 1, 5–25%; 2, 25–50%; 3, 51–75%; and 4, >75%) multiplied by the immunostaining intensity (range: 0–4; 0, non-staining; 1, low intensity; 2 median intensity; and 3, high intensity).

Cell proliferation and migration assays

The stably transfected A375 were divided into different groups and seeded onto a 96-well plate at a density of 5×10^4 cells/ml. We used the Cell Counting Kit-8 (CCK-8 Kit; Dojindo, Japan), based on the manufacturer's instructions, to determine the proliferative capacity of cells. Optical density (OD) values were obtained at 450 nm after 24, 48, 72, 96, and 120 h. A transwell cell migration assay was used to test the ability of cells to metastasize. The cell density of different groups was adjusted to 2×10^5 cells/ml, and 100 μl cell suspension of different groups was added to the upper chamber with or without Matrigel

(Corning, United States). The cells were cultured for 48 h in a humidified incubator containing 5% CO_2 at 37°C . The cells were then removed, fixed with 4% paraformaldehyde for 30 min, washed 3 times with PBS, stained with 1% crystal violet for 30 min, and rewashed with PBS. Each sample was viewed and photographed under a microscope in 5 fields. Crystal violet was eluted with 300 μl of 33% acetic acid, and 100 μl cell suspension of different groups was added to each of the 96-well plates. OD value at 450 nm was determined. Migrated cells were imaged in a randomly chosen field of view and counted utilizing the $\times 200$ microscope.

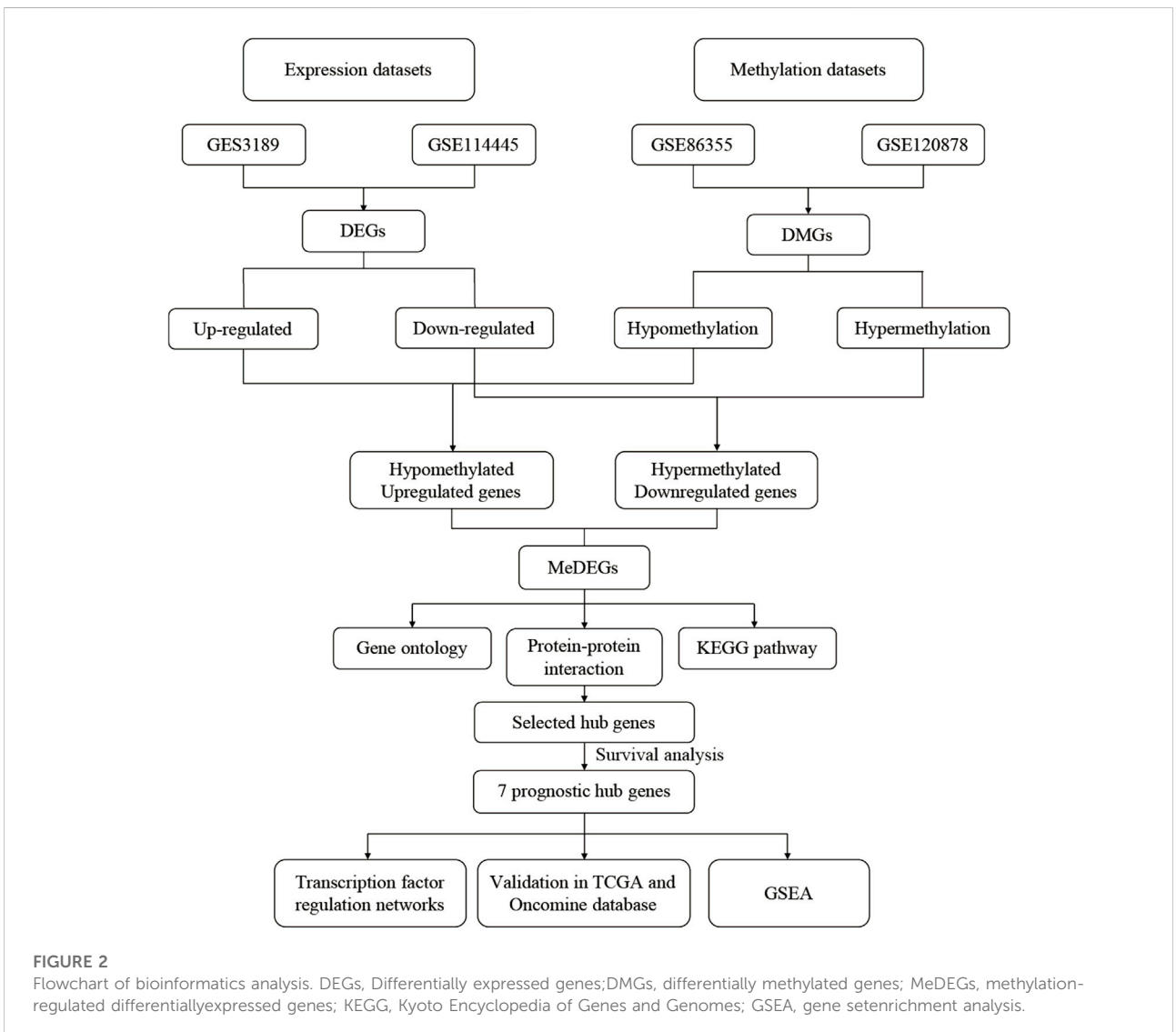
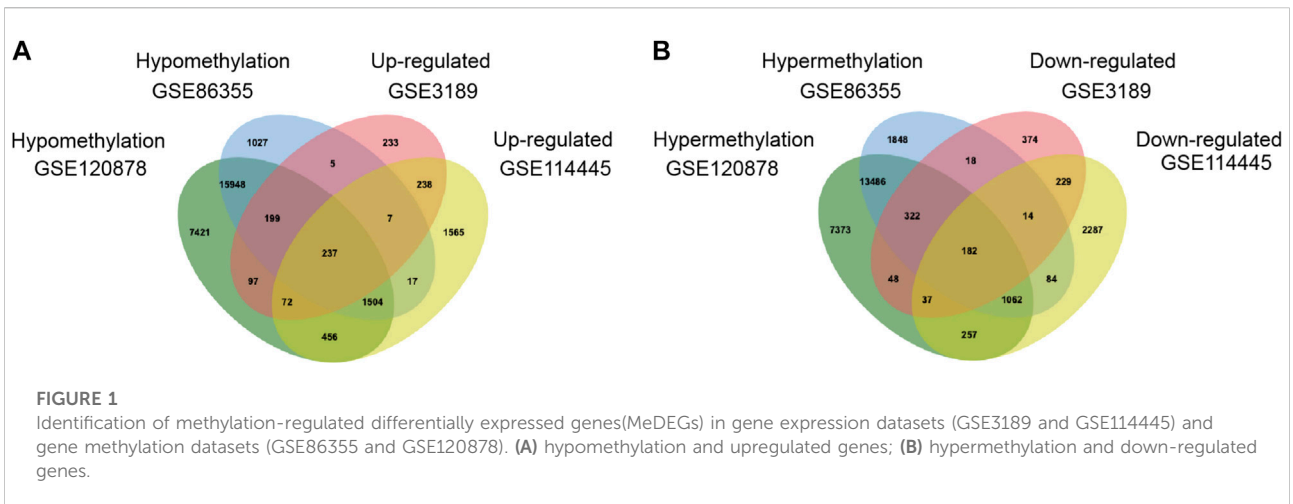
Results

Identification of methylation-regulated differentially expressed genes in skin cutaneous melanoma

GEO2R was adopted to identify the DEGs and DMGs, respectively. For DEGs of gene expression microarray, 554 overlapping up-regulated genes (1,088 in GSE3189, 4,096 in GSE114445) and 462 overlapping down-regulated genes (1,224 in GSE3189, 4,152 in GSE114445) were screened. For DMGs of gene methylation microarray, 15,052 overlapping hypermethylation genes (17,016 in GSE86355, 22,767 in GSE120878) and 17,888 overlapping hypomethylation genes (18,944 in GSE86355, 25,934 in GSE120878) were found. As shown in [Figure 1](#), we identified 237 hypomethylated, upregulated genes and 182 hypermethylated, downregulated genes after integrating the DEGs and DMGs. The flowchart was illustrated in [Figure 2](#). The representative heat map of the MeDEGs of GSE3189 (including the top 50 up-regulated and down-regulated genes) was present in [Figure 3](#).

Functional enrichment analysis of methylation-regulated differentially expressed genes

The results of the GO enrichment analysis for the MeDEGs were shown in [Tables 1, 2](#). For hypomethylation-upregulated genes, changes in biologic processes were mostly enriched in the oxidation-reduction process, cell proliferation, cell division, phosphorylation, extracellular matrix disassembly and protein sumoylation. The hypermethylation-downregulated genes were mainly enriched in positive regulation of transcription from RNA polymerase II promoter, cell adhesion, cell proliferation, positive regulation of transcription, DNA-templated and angiogenesis. We also found that the hypomethylated, upregulated genes were related to cytosol, extracellular



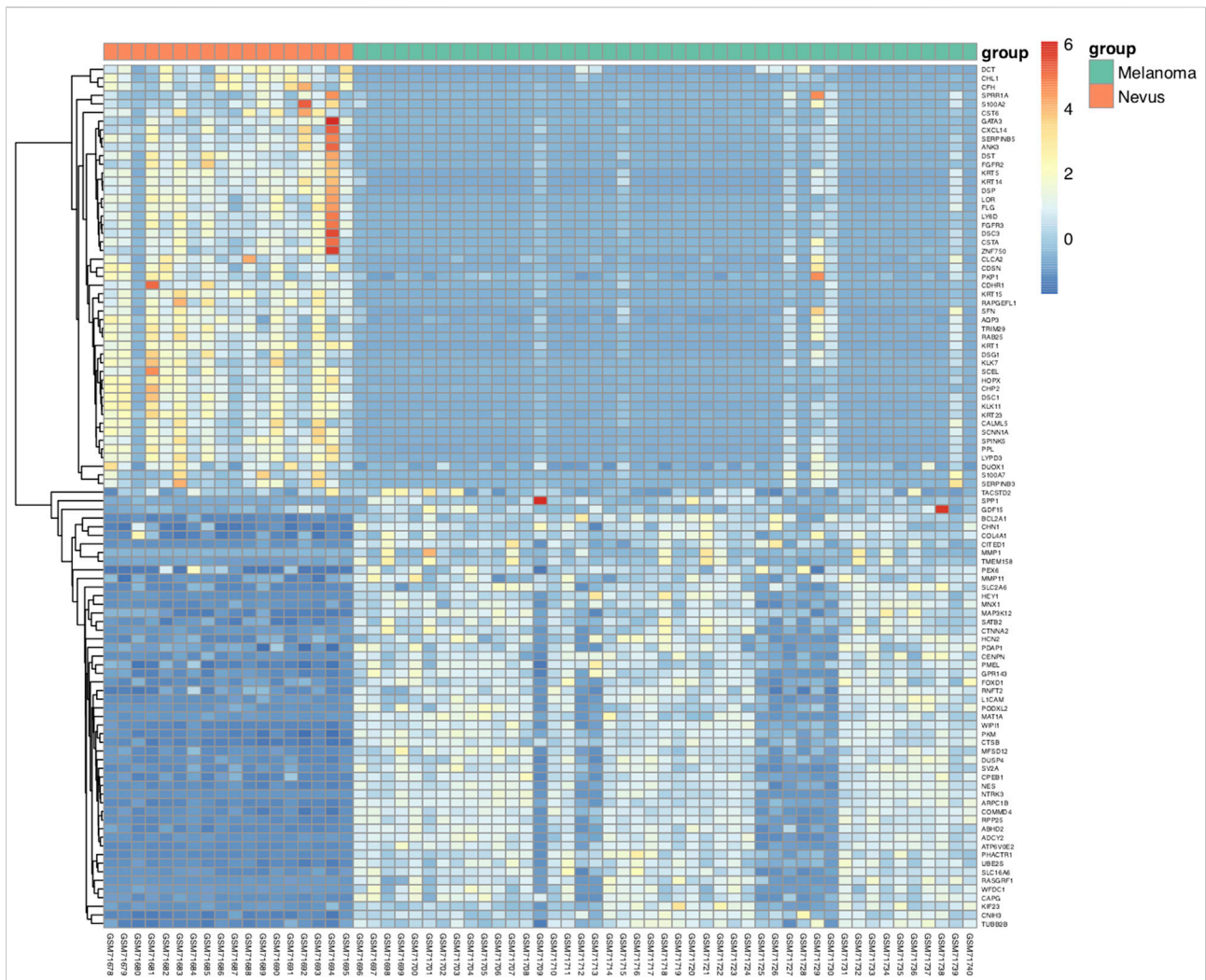


FIGURE 3 Representative heat map of the top 100 differentially expressed genes in dataset GSE3189 (50 up-regulated genes and 50 down-regulated genes). Red: upregulation; blue: down-regulation.

exosome, membrane and nucleoplasm, while hypermethylated, downregulated genes to cytoplasm, plasma membrane, cytosol and cell junction in the cellular component group. For hypomethylated, upregulated genes, changes in molecular function were primarily enriched in protein binding, ATP binding, enzyme binding and GTPase activity, and for hypermethylated, downregulated genes, changes were significantly enriched in protein binding, transcriptional activator activity, RNA polymerase II core promoter proximal region sequence-specific binding and transcription factor activity, sequence-specific DNA binding. Pathway enrichment was also performed using KEGG, and the results were shown in Table 3. We found that hypomethylated genes predominantly participated in selenocompound metabolism, small cell lung cancer and

lysosome. For hypermethylated genes, the most significantly enriched pathways involved the transcriptional misregulation in cancer, circadian rhythm, tight junction, protein digestion and absorption and Hippo signaling pathway.

Protein-protein interaction network establishment and hub genes selection

The PPI network of hypomethylation-upregulated genes and hypermethylation-downregulated genes was visualized by Cytoscape (version 3.6.0) (Smoot et al., 2011). MCODE (version 1.4.2) is a plug-in of Cytoscape to cluster a given network to select densely connected

TABLE 1 Gene ontology enrichment analysis of hypomethylated upregulated genes.

| Category | Term | Description | Count | p-Value |
|----------|------------|--|-------|----------|
| BP | GO:0001887 | selenium compound metabolic process | 3 | 1.68E-03 |
| BP | GO:0016310 | phosphorylation | 7 | 2.07E-03 |
| BP | GO:0022617 | extracellular matrix disassembly | 6 | 3.27E-03 |
| BP | GO:0000059 | protein import into nucleus, docking | 3 | 4.58E-03 |
| BP | GO:0060236 | regulation of mitotic spindle organization | 3 | 4.58E-03 |
| BP | GO:0006606 | protein import into nucleus | 5 | 7.11E-03 |
| BP | GO:0016925 | protein sumoylation | 6 | 1.93E-02 |
| BP | GO:0008283 | cell proliferation | 11 | 2.33E-02 |
| BP | GO:0051301 | cell division | 10 | 4.25E-02 |
| BP | GO:0055114 | oxidation-reduction process | 14 | 4.98E-02 |
| CC | GO:0016020 | membrane | 59 | 2.73E-08 |
| CC | GO:0070062 | extracellular exosome | 67 | 1.96E-07 |
| CC | GO:0005829 | cytosol | 75 | 2.01E-07 |
| CC | GO:0031012 | extracellular matrix | 15 | 2.53E-05 |
| CC | GO:0005654 | nucleoplasm | 54 | 1.16E-03 |
| CC | GO:0005783 | endoplasmic reticulum | 22 | 1.90E-03 |
| CC | GO:0031965 | nuclear membrane | 10 | 2.60E-03 |
| CC | GO:0005925 | focal adhesion | 13 | 4.18E-03 |
| CC | GO:0001772 | immunological synapse | 4 | 8.90E-03 |
| CC | GO:0042470 | melanosome | 6 | 9.11E-03 |
| CC | GO:0043231 | intracellular membrane-bounded organelle | 15 | 1.16E-02 |
| CC | GO:0005789 | endoplasmic reticulum membrane | 19 | 2.54E-02 |
| CC | GO:0005737 | cytoplasm | 79 | 4.60E-02 |
| CC | GO:0005794 | Golgi apparatus | 18 | 4.67E-02 |
| CC | GO:0005739 | mitochondrion | 25 | 4.91E-02 |
| MF | GO:0005515 | protein binding | 149 | 7.15E-05 |
| MF | GO:0008139 | nuclear localization sequence binding | 4 | 6.28E-03 |
| MF | GO:0005524 | ATP binding | 32 | 1.15E-02 |
| MF | GO:0003924 | GTPase activity | 9 | 1.47E-02 |
| MF | GO:0019899 | enzyme binding | 11 | 1.58E-02 |
| MF | GO:0051015 | actin filament binding | 6 | 3.40E-02 |

regions based on topology (Bandettini et al., 2012). The results were presented in Figure 4. Therefore, PBK, TK1, TACC3, MYBL2, TPX2, DTL, KPNA2, KIF2C, CKS2, ASF1B, SPAG5 and NCAPH were verified as hub genes in hypomethylation-upregulated genes module. And EIF4B, EIF3L, EIF3A, RPS7, RPL22, RSL1D1, RPS23, RPL11 and FBL were selected as hub genes in the hypermethylation-downregulated genes module.

Survival analysis

Significant survival outcomes of hub genes in the PPI network were displayed in Figure 5. According to the expression of each gene, overall survival for SKCM patients was acquired. We found that high mRNA expression of CKS2

($p = 0.033$) was closely related to worse prognosis for SKCM as well as DTL ($p = 0.00096$), KIF2C ($p = 0.01$), KPNA2 ($p = 0.0017$), MYBL2 ($p = 0.0022$), TPX2 ($p = 0.0074$), FBL ($p = 0.0013$).

Hub genes verification

Subsequently, we used the OncoPrint database to further validate the expression of seven hub genes. The different expression levels of six hypomethylated upregulated hub genes and one hypermethylated downregulated hub genes between melanoma and nevus samples were significantly obvious (Figure 6), which were consistent with the results we obtained.

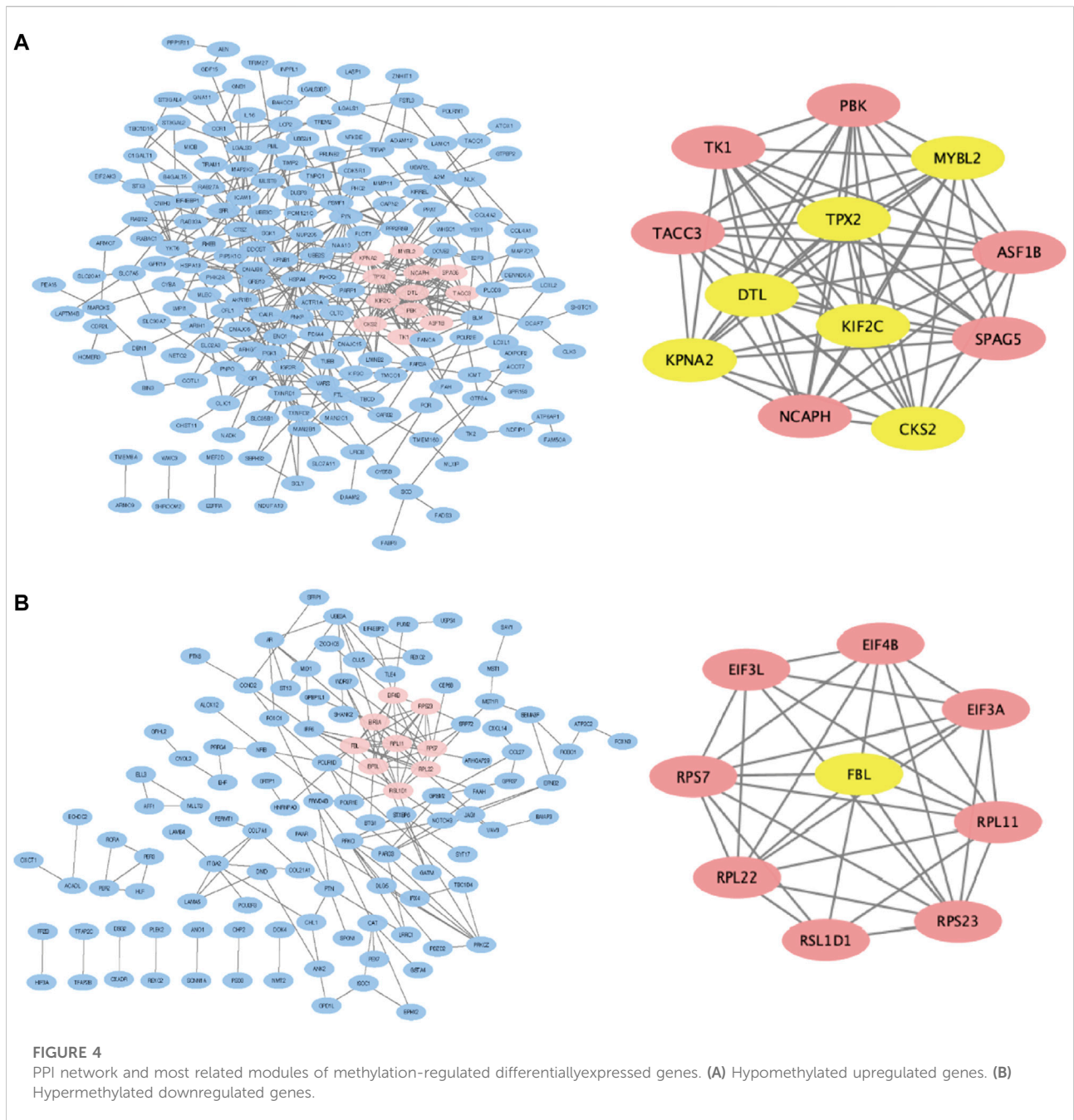
In addition, we used the cBioPortal tool to explore the genetic alterations of seven hub genes and discovered that

TABLE 2 Gene ontology enrichment analysis of hypermethylated downregulated genes.

| Category | Term | Description | Count | p-Value |
|----------|------------|---|-------|----------|
| BP | GO:0007155 | cell adhesion | 15 | 2.30E-04 |
| BP | GO:0001954 | positive regulation of cell-matrix adhesion | 4 | 1.34E-03 |
| BP | GO:0045944 | positive regulation of transcription from RNA polymerase II promoter | 21 | 2.07E-03 |
| BP | GO:0050680 | negative regulation of epithelial cell proliferation | 5 | 2.42E-03 |
| BP | GO:0006366 | transcription from RNA polymerase II promoter | 13 | 5.80E-03 |
| BP | GO:0090162 | establishment of epithelial cell polarity | 3 | 6.22E-03 |
| BP | GO:0001942 | hair follicle development | 4 | 6.52E-03 |
| BP | GO:0001525 | angiogenesis | 8 | 7.46E-03 |
| BP | GO:0008284 | positive regulation of cell proliferation | 12 | 7.63E-03 |
| BP | GO:0016477 | cell migration | 7 | 7.97E-03 |
| BP | GO:0008285 | negative regulation of cell proliferation | 10 | 1.90E-02 |
| BP | GO:0090090 | negative regulation of canonical Wnt signaling pathway | 6 | 2.46E-02 |
| BP | GO:0008283 | cell proliferation | 9 | 3.21E-02 |
| BP | GO:0042493 | response to drug | 8 | 3.44E-02 |
| BP | GO:0045893 | positive regulation of transcription, DNA-templated | 11 | 3.57E-02 |
| CC | GO:0016324 | apical plasma membrane | 13 | 3.17E-05 |
| CC | GO:0005911 | cell-cell junction | 8 | 1.57E-03 |
| CC | GO:0005737 | cytoplasm | 70 | 2.63E-03 |
| CC | GO:0005856 | cytoskeleton | 10 | 1.12E-02 |
| CC | GO:0005829 | cytosol | 46 | 1.22E-02 |
| CC | GO:0030054 | cell junction | 11 | 1.55E-02 |
| CC | GO:0031012 | extracellular matrix | 8 | 2.73E-02 |
| CC | GO:0005886 | plasma membrane | 52 | 3.85E-02 |
| CC | GO:0005925 | focal adhesion | 9 | 3.96E-02 |
| MF | GO:0001077 | transcriptional activator activity, RNA polymerase II core promoter proximal region sequence-specific binding | 10 | 5.79E-04 |
| MF | GO:0005515 | protein binding | 106 | 2.94E-03 |
| MF | GO:0000989 | transcription factor activity, transcription factor binding | 3 | 8.19E-03 |
| MF | GO:0008013 | beta-catenin binding | 5 | 8.89E-03 |
| MF | GO:0043565 | sequence-specific DNA binding | 12 | 1.41E-02 |
| MF | GO:0003700 | transcription factor activity, sequence-specific DNA binding | 17 | 2.88E-02 |

TABLE 3 Pathway enrichment analysis of MeDEGs.

| Category | Term | Count | p-Value |
|-------------------------------------|--|-------|----------|
| Hypomethylated upregulated genes | | | |
| KEGG_PATHWAY | hsa00450:Selenocompound metabolism | 4 | 2.42E-03 |
| KEGG_PATHWAY | hsa05222:Small cell lung cancer | 6 | 1.22E-02 |
| KEGG_PATHWAY | hsa04142:Lysosome | 6 | 4.70E-02 |
| Hypermethylated downregulated genes | | | |
| KEGG_PATHWAY | hsa05202:Transcriptional misregulation in cancer | 6 | 3.51E-02 |
| KEGG_PATHWAY | hsa04710:Circadian rhythm | 3 | 4.45E-02 |
| KEGG_PATHWAY | hsa04530:Tight junction | 4 | 6.89E-02 |
| KEGG_PATHWAY | hsa04974:Protein digestion and absorption | 4 | 7.08E-02 |
| KEGG_PATHWAY | hsa04390:Hippo signaling pathway | 5 | 8.21E-02 |

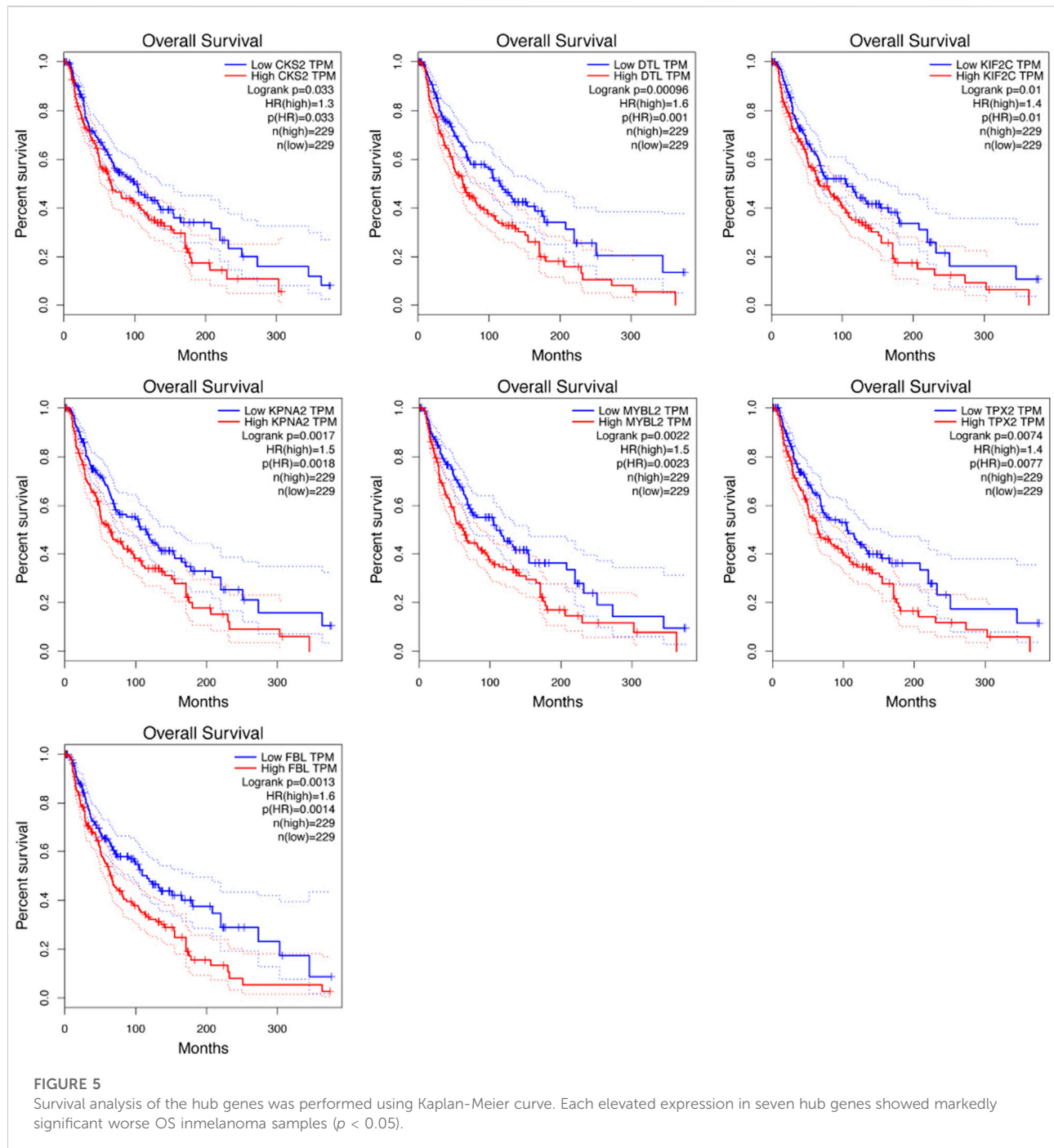


DTL (17%) and KIF2C (13%) were the most frequently altered genes among the seven hub genes, including amplification, fusion, and missense mutations (Figures 7A,B). The alterations of the seven hub genes were 192 (43.24%) of 444 sequenced cases/patients. The correlations between mRNA and DNA methylation of the seven genes in the TCGA SKCM patients were demonstrated in Figure 7C. We found that the correlation was negative, indicating that methylation regulated the mRNA expression of these genes.

This illustrated that methylation played an important role in the expression of these genes.

Significant genes and pathways obtained by gene set enrichment analysis

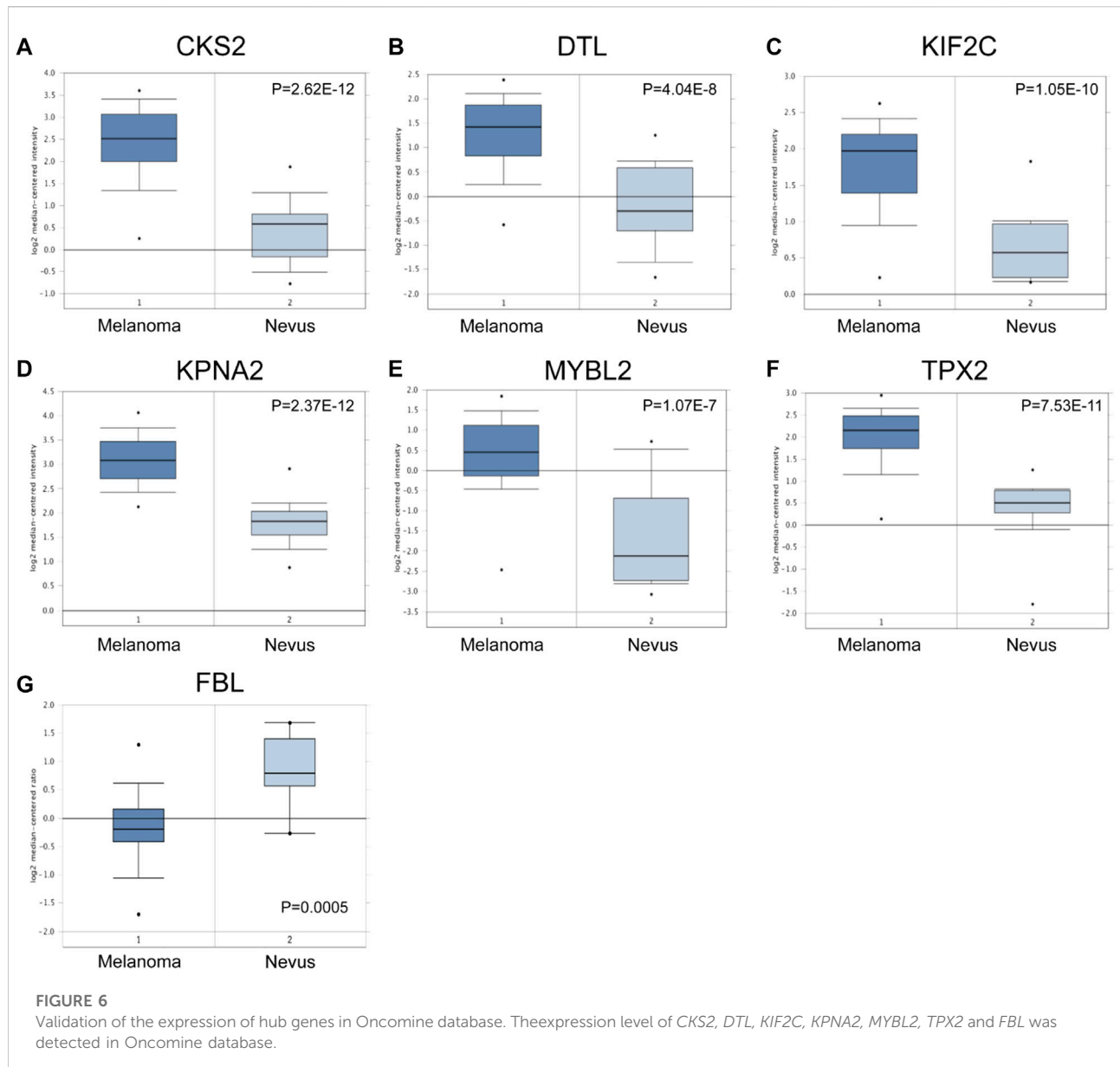
Transcriptional regulation networks among *CKS2*, *DTL*, *KIF2C*, *KPNA2*, *MYBL2*, *TPX2* and *FBL* were displayed in Figure 8.



Significantly involved nodes (including transcription factor regulation-DNA binding, related lncRNA, targeted miRNA and protein-protein interaction) were marked in different colors. Subsequently, a total of 100 significant genes were obtained from GSEA, and the genes with positive correlations were plotted. GSEA analysis, including *CKS2*, *DTL*, *KIF2C*, *KPNA2*, *MYBL2*, and *TPX2* indicated that the most involved hallmarks pathways were E2F targets, G2M checkpoint and mitotic spindle. The details were illustrated in Figure 9.

Kinesin family member 2C expression pattern and its pro-tumorigenic malignant biological behaviors in skin cutaneous melanoma

To reveal levels of expression and methylation of KIF2C in SKCM samples, we first enrolled 33 SKCM tissues and assessed the protein expression of KIF2C in SKCM using IHC analysis

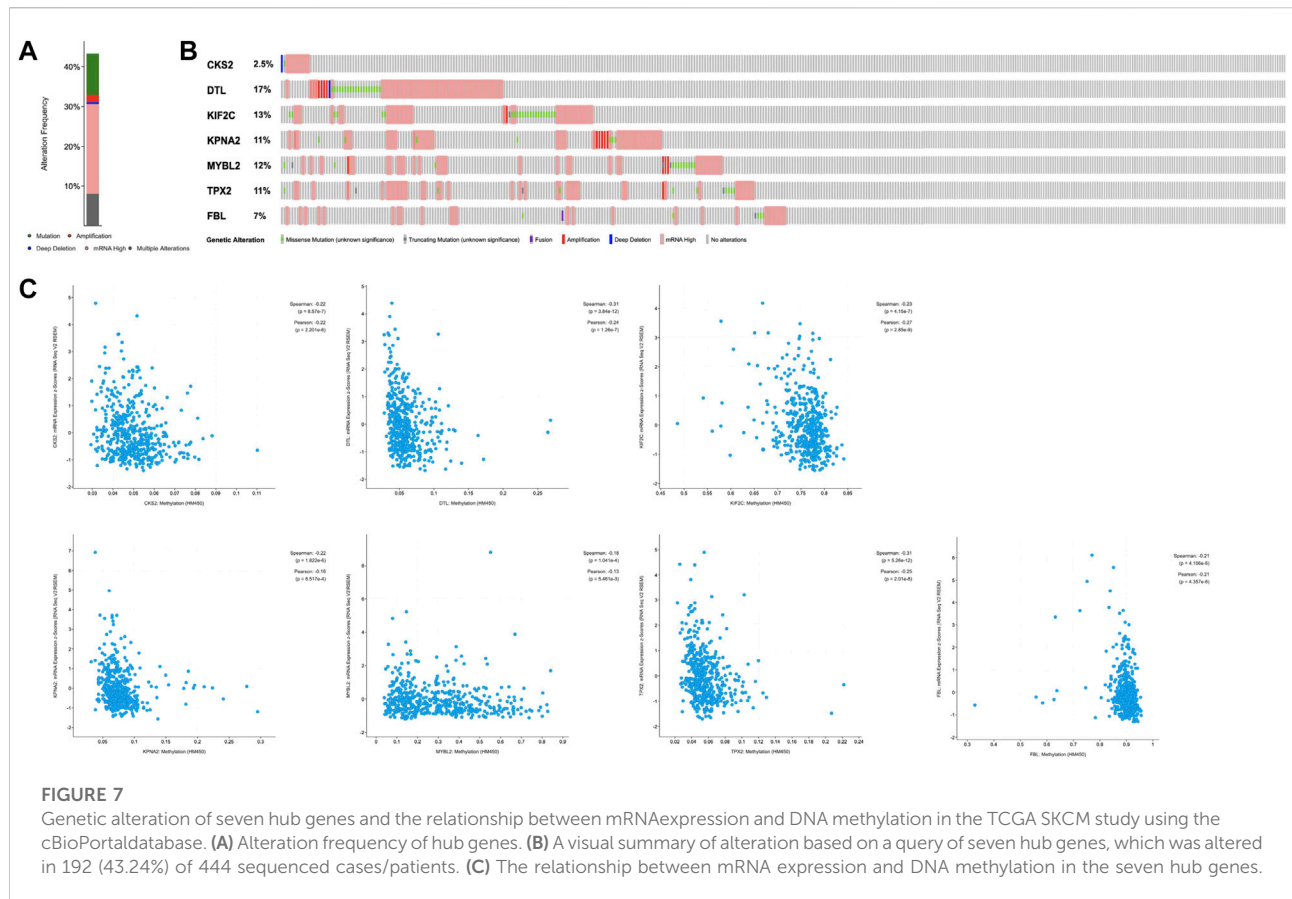


(Supplementary Figure S1A). Methylation-specific PCR was used to detect the methylation expression of *KIF2C*. Pearson correlation analysis suggested showed a significantly negative association between the protein and methylation expression ($r = -0.362$, $p < 0.001$) (Supplementary Figure S1B). Then, qRT-PCR was used to detect the knockdown efficacy of siRNAs silencing the expression of *KIF2C* in A375 cells. Significantly, compared with the negative control group, transcriptional expression of *KIF2C* was decreased in siRNA1- and siRNA2-treated groups. Therefore, siRNA1 and siRNA2 were used for further experiments (Supplementary Figure S1C). According to the results of the CCK-8 assay, the

down-regulated level of *KIF2C* expression significantly inhibited the proliferative ability of SKCM cells (Supplementary Figure S1D). Transwell cell migration assay indicated that the down-expression of *KIF2C* suppressed the metastasis capacity of SKCM cells (Supplementary Figure S1E).

Discussion

Melanoma is an aggressive and devastating cancer that can be directly derived from melanocytic nevus. Nowadays, surgery of tumor resection before metastasis still remains the most effective

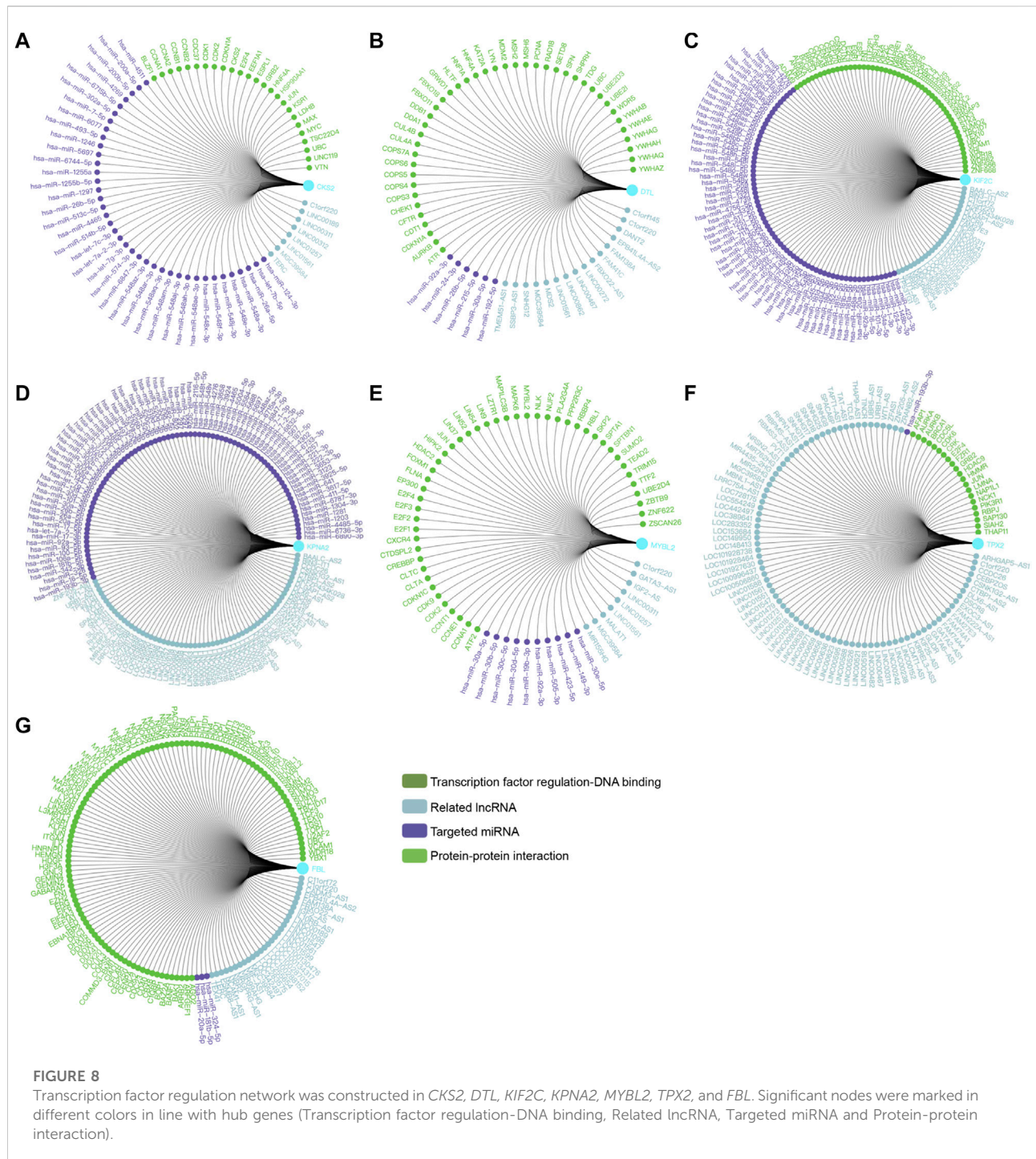


treatment (Gadeliya Goodson and Grossman, 2009). Thus, it is important to diagnose the high-risk nevus in the early stage. Identification of novel biomarkers will be greatly helpful to improve diagnosis and an even better understanding of the mechanism involved in melanocytic tumorigenesis that potentially contributes to novel therapy. Hence, highly effective biomarkers for diagnosis and treatment are urgently required.

The initiation and progression involved in melanoma is a complicated and multistage process regulated by both genetic and epigenetic alterations. Increasing evidence has shown the essential roles of epigenetic modifications, especially DNA methylation, in SKCM (Schinke et al., 2010; Berger et al., 2012; Goran Micevic et al., 2017). However, most of these studies are limited to melanoma metastases and lack primary melanomas, which made it difficult to identify early biological progress during melanoma development (Weiyang Cai et al., 2018). Furthermore, separate analyses of gene expression and methylation from one study are limited (Wouters et al., 2017), while integrating multiple available datasets may help us find more accurate and reliable evidence through comprehensive bioinformatics analysis. Yet, conjoint

analysis including both gene expression and methylation profiling microarray datasets is largely insufficient in SKCM. Therefore, we conducted an integrated bioinformatics analysis based on both gene expression and gene methylation profiling to identify the new prognostic biomarkers and therapeutic targets in SKCM for future research.

In the present study, we identified a total of 237 hypomethylated, upregulated genes and 182 hypermethylated, downregulated genes by overlapping the DEGs and DMGs. For the hypomethylation-upregulated genes, functional enrichment analysis indicated that changes in the biological processes were mainly enriched in the oxidation-reduction process, cell proliferation, cell division, phosphorylation, extracellular matrix disassembly and protein sumoylation. GO cell component analysis showed that the upregulated genes were significantly enriched in cytosol, extracellular exosome, membrane and nucleoplasm. In addition, for molecular function, the hypomethylation-upregulated genes were significantly enriched in protein binding, ATP binding, enzyme binding and GTPase activity. KEGG pathway enrichment analysis suggested significant



enrichment in pathways including selenocompound metabolism, small cell lung cancer and lysosome. Notably, GSEA results showed that E2F targets, G2M checkpoint and mitotic spindle were the most involved hallmarks in SKCM. These findings are reasonable because it is universally acknowledged that the above

processes are closely related to tumor initiation and progression, including melanoma (Hanahan and Weinberg Robert, 2011).

PPI network of hypomethylation-high expression genes illustrated the protein-protein interactome of the hub genes, and then GEPIA was adopted to select the most prognostic

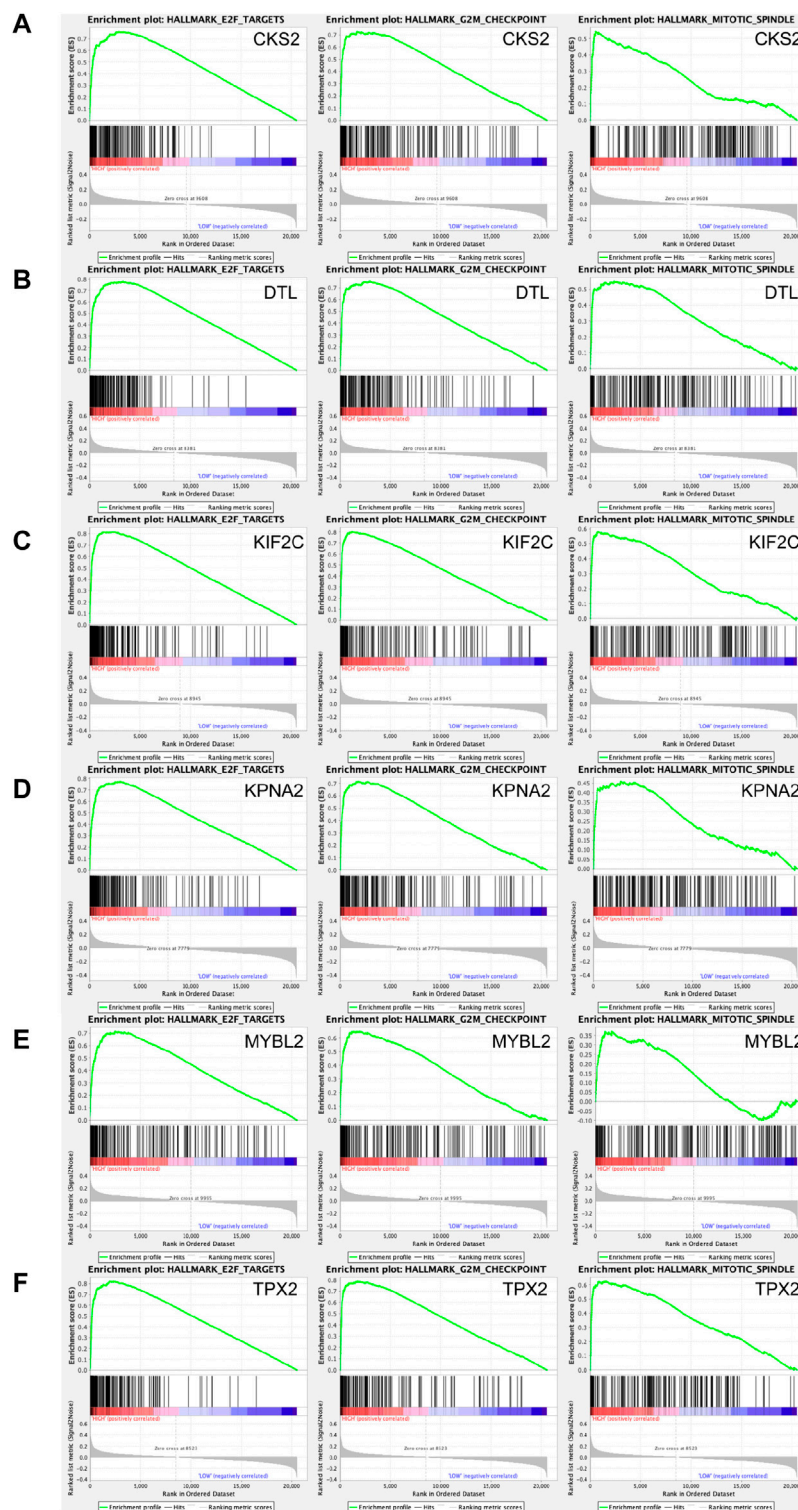


FIGURE 9

A total of 100 significant genes were obtained from GSEA with positive and negative correlations. GSEA was used to perform hallmark analyses in *CKS2*, *DTL*, *KIF2C*, *KPNA2*, *MYBL2* and *TPX2*, respectively. The most involved significant pathways included E2F targets, G2M checkpoint and mitotic spindle.

hub genes, named *CKS2*, *DTL*, *KIF2C*, *KPNA2*, *MYBL2* and *TPX2*, which may provide new clues for the therapeutic strategy in SKCM.

Cyclin-dependent kinases regulatory subunit 2 (*CKS2*), a cyclin-dependent kinase-interacting protein, is critical for cell cycle regulation. Overexpression of *CKS2* has been reported to be associated with several types of cancer, including colorectal cancer and cervical cancer (Yu et al., 2015; Jonsson et al., 2019). de Wit et al. (2005) reported that *CKS2* could be considered a candidate player in melanocytic tumor progression and facilitate early diagnosis of melanocytic lesions before metastasis. We found that the expression of *CKS2* in SKCM tissues was higher in different datasets, and survival analysis revealed that the upregulation of *CKS2* was related to a worse prognosis in SKCM, which was consistent with the results of previous studies.

Denticleless E3 ubiquitin protein ligase homologue (*DTL*), also known as DNA replication factor 2, can regulate the expression of various cell cycle regulatory proteins and maintain the integrity of DNA replication and repair (Pan et al., 2006). Elevated expression of *DTL* has been found to be related to a variety of cancers, such as breast cancer, Ewing sarcoma and ovarian cancer (Ueki et al., 2008; Mackintosh et al., 2012; Pan et al., 2013). Yang et al. (2019) suggested that *DTL* can be regarded as an indicator of poor prognosis in acral melanoma patients. *DTL* could play an important role in promoting melanoma cell growth and glucose metabolism, possibly through activation of the *MYC* target pathway (Lu et al., 2022). In the present study, we found that overexpressed *DTL* was closely associated with worse survival outcomes in cutaneous melanoma patients. The rate of *DTL* mutation was 17%, and this higher mutation rate may lead to abnormal methylation or deregulation of *DTL*.

As a member of the kinesin-13 family, kinesin family member 2C (*KIF2C*) uses microtubule depolymerizing activity to correct improper microtubule attachments at kinetochores, which plays significant roles during the mitosis process (Lawrence et al., 2004; Gardner Melissa et al., 2011). *KIF2C* is likely to be the essential gene for carcinogenesis and may be closely involved in tumor-infiltrating lymphocytes of cancer immunotherapy for patients with metastatic melanoma (Lu et al., 2014). In our study, we found that the expression of *KIF2C* was significantly elevated in SKCM tissues compared to nevus tissues and associated with poor prognosis in melanoma patients by bioinformatic research. Importantly, we validated that the down-regulated level of *KIF2C* expression significantly inhibited the proliferative ability and suppressed the metastasis capacity of SKCM cells.

KPNA2, a member of karyopherin (*KPNA*) protein family, is considered as a key role in the malignant transformation of cells through the transport of tumor suppressors, regulation of DNA repair proteins as well as activation of apoptosis pathways (Tseng et al., 2005). Elevated *KPNA* levels have

been found to predict poor prognosis for multiple tumors, including breast and cervical cancer (Dahl et al., 2006; van der Watt et al., 2009). Winnepenninckx et al. (2006) reported that *KPNA2* is closely associated with poor prognosis and tumor progression in melanoma, which is consistent with our results. Yang et al. (2020) found that *KPNA2* promotes proliferation, invasion and migration through NF- κ B/p65 signaling pathways in melanoma cells. In this study, we suggested the possibility of the aberrant methylation of the *KPNA2* promoter.

Myb proto-oncogene like 2 (*MYBL2*), located on chromosome 20q13, acts as a transcription factor that plays a significant role in cell-cycle progression. In the previous study, overexpression of *MYBL2* has been found to be related to poor prognosis in various cancers, such as prostate and gallbladder cancer (Bar-Shira et al., 2002; Liang et al., 2017). Koynovaa et al. (2007) found a higher frequency of low-level increase of the copy numbers of *MYBL2* rather than amplification in melanoma. Also, evidence showed that attenuation of miR-29b2~c expression promotes the development of melanoma by partly depressing MAFG and *MYBL2* (Vera et al., 2021). Taken together, this evidence indicated that *MYBL2* was involved in cell proliferation and tumorigenesis in melanoma, which is consistent with our present findings. However, further research is needed to confirm our hypothesis.

Targeting protein for xenopus kinesin-like protein 2 (*TPX2*, also known as REPP86) located on chromosome 20q11.2 in humans. *TPX2* is a mitotic microtubule-associated protein that is strictly regulated by the cell cycle and diffusely distributed during the S and G2 phases, which help spindle stability (Alfaro-Aco and Petry, 2017). Ping Wei et al. (2013) demonstrated that upregulation of *TPX2* was associated with the clinical stage, invasion and metastasis in colon cancer, participating in the P13K/Akt signaling pathway to reduce the occurrence as well as the proliferation of colon cancer cells. Increased expression of *TPX2* was also observed in lung squamous cell carcinoma, ovarian cancer and giant-cell tumor of the bone (Ignacio Blanco et al., 2015; Laura et al., 112006; Aguirre-Portoles et al., 2012). Yao et al. (2018) showed that *TPX2* improved the proliferative ability of melanoma cell lines and functioned as an oncogene in melanoma. In our study, *TPX2* was found to be a hypomethylated-upregulated gene in melanoma and associated with the poor prognostic of melanoma patients, which suggested that *TPX2* may be used as a novel prognostic marker for the development and progression of SKCM. Our results were consistent with the roles of *TPX2* in various tumors reported in previous studies.

As for the hypermethylation-downregulated genes, functional enrichment analysis indicated that changes in biological processes were mainly enriched in the positive

regulation of transcription from RNA polymerase II promoter, cell adhesion, cell proliferation, positive regulation of transcription, DNA-templated and angiogenesis. GO cell component analysis showed that the downregulated genes were significantly enriched in the cytoplasm, plasma membrane, cytosol and cell junction. Besides, for molecular function, the hypermethylation-downregulated genes were significantly enriched in protein binding, transcriptional activator activity, RNA polymerase II core promoter proximal region sequence-specific binding and transcription factor activity, and sequence-specific DNA binding. KEGG pathway enrichment analysis suggested significant enrichment in pathways including transcriptional misregulation in cancer, circadian rhythm, tight junction, protein digestion and absorption and Hippo signaling pathway. Importantly, growing evidence showed that numerous genetic changes in melanoma may be linked to in Hippo signaling pathway (Kim et al., 2013; Feng et al., 2017). Moreover, Hippo pathway was found to be correlated with the mitogen-activated protein kinase (MAPK) signaling pathway which is well known for a vital role in the pathogenesis of melanoma (Feng et al., 2017).

Then, we performed a PPI network and survival analysis to identify the prognostic hub gene among the hypermethylation-downregulated genes. Fibrillarin (FBL) is an indispensable, highly conserved protein essential in the processing of pre-rRNAs (Newton et al., 2003). In the previous study, the expression of FBL can be regulated by p53 in multiple tumors and was considered as an ideal target to inhibit the ribosome biogenesis process in cancer therapy (Marcel et al., 2013; El Hassouni et al., 2019). Overexpression of FBL was found in breast, prostate cancers and squamous cell cervical carcinoma (Choi et al., 2007; Koh et al., 2011; Su et al., 2014). Thus, FBL could have a role in tumor progression and could affect the clinical outcome of patients through alteration of translational regulation in melanoma. In our study, we found that the low expression of FBL in SKCM tissues compared to nevus tissues was observed in multiple datasets, and survival analysis showed that the high expression of FBL was related to a worse prognosis in SKCM.

The present study constructed a comprehensive network between nevus and melanoma and identify the prognostic significance of these hub genes, which may serve as valuable prognostic indicators of SKCM. However, there are still some limitations in this study: firstly, the gene expressions and methylation profiles were from different studies (Wu et al., 2018); secondly, the survival outcomes might be heavily contaminated due to cancer subtypes (Ren et al., 2019), thus the result could be not very stable. Furthermore in-depth investigation through *in vivo* and *in vitro* experimental designs and analyses are needed in future work.

Conclusion

In summary, this study identified methylation-regulated differentially expressed genes and related pathways and functions in SKCM by using integrated bioinformatics analysis. In addition, we constructed PPI networks and performed survival analysis that identified seven prognostic hub genes. Our findings may deepen the understanding of the methylation-mediated regulatory mechanisms underlying the carcinogenesis possibility of melanocytic nevus and melanoma and provide novel biomarkers and therapeutic targets for further research.

Author contributions

The work presented here was carried out in collaboration among all authors. G-LS defined the research theme, discussed analyses, interpretation, and presentation. C-HH, WH and Y-ZW drafted the manuscript, analyzed the data, developed the algorithm and interpreted the results. All authors read and approved the final manuscript.

Conflict of interest

The authors declare that the research was conducted in the absence of any commercial or financial relationships that could be construed as a potential conflict of interest.

Publisher's note

All claims expressed in this article are solely those of the authors and do not necessarily represent those of their affiliated organizations, or those of the publisher, the editors and the reviewers. Any product that may be evaluated in this article, or claim that may be made by its manufacturer, is not guaranteed or endorsed by the publisher.

Supplementary material

The Supplementary Material for this article can be found online at: <https://www.frontiersin.org/articles/10.3389/fgene.2022.817656/full#supplementary-material>

SUPPLEMENTARY FIGURE S1

Validation of the KIF2C role in SKCM. (A) IHC analysis was performed to reveal high expression of KIF2C in SKCM samples. (B) Methylation specific PCR was used to detect the methylation expression of KIF2C. Pearson correlation analysis suggested showed significantly negative association between the protein and methylation expression ($r = -0.362$, $p < 0.001$). (C) qRT-PCR was used to detect the knockdown efficacy of siRNAs silencing expression of KIF2C in A375 cells. Significantly,

compared with the negative control group, transcriptional expression of KIF2C was decreased in siRNA1- and siRNA2-treated groups. (D) According to the results of the CCK-8 assay, down-regulated level of

KIF2C expression significantly inhibited the proliferative ability of SKCM cells. (E) Transwell cell migration assay indicated that the down-expression of KIF2C suppressed metastasis capacity of SKCM cells.

Reference

- Aguirre-Portoles, C., Bird, A. W., Hyman, A., Canamero, M., Perez de Castro, I., Malumbres, M., et al. (2012). Tpx2 controls spindle integrity, genome stability, and tumor development. *Cancer Res.* 72 (6), 1518–1528. doi:10.1158/0008-5472.CAN-11-1971
- Alfaro-Aco, R., and Petry, S. (2017). How TPX2 helps microtubules branch out. *Cell Cycle* 16 (17), 1560–1561. doi:10.1080/15384101.2017.1348080
- Ashburner, M., Ball, C. A., Blake, J. A., Botstein, D., Butler, H., Cherry, J. M., et al. (2000). Gene ontology: Tool for the unification of biology. The gene ontology consortium. *Nat. Genet.* 25 (1), 25–29. doi:10.1038/75556
- Bandettini, W. P., Kellman, P., Mancini, C., Booker, O. J., Vasu, S., Leung, S. W., et al. (2012). MultiContrast delayed enhancement (MCOE) improves detection of subendocardial myocardial infarction by late gadolinium enhancement cardiovascular magnetic resonance: A clinical validation study. *J. Cardiovasc. Magn. Reson.* 14, 83. doi:10.1186/1532-429X-14-83
- Bar-Shira, AnatJ. H. P., Rozovsky, Uri, Goldstein, Myriam, Sellers, William R., Yaron, Yuval, Eshhar, Zelig, et al. (2002). Multiple genes in human 20q13 chromosomal region are involved in an advanced prostate cancer xenograft. *Cancer Res.* 62, 6803–6807.
- Berger, M. F., Hodis, E., Heffernan, T. P., Deribe, Y. L., Lawrence, M. S., Protopopov, A., et al. (2012). Melanoma genome sequencing reveals frequent PREX2 mutations. *Nature* 485 (7399), 502–506. doi:10.1038/nature11071
- Cerami, E., Gao, J., Dogrusoz, U., Gross, B. E., Sumer, S. O., Aksoy, B. A., et al. (2012). The cBio cancer genomics portal: An open platform for exploring multidimensional cancer genomics data. *Cancer Discov.* 2 (5), 401–404. doi:10.1158/2159-8290.CD-12-0095
- Choi, Y. W., Kim, Y. W., Bae, S. M., Kwak, S. Y., Chun, H. J., Tong, S. Y., et al. (2007). Identification of differentially expressed genes using annealing control primer-based GeneFishing in human squamous cell cervical carcinoma. *Clin. Oncol.* 19 (5), 308–318. doi:10.1016/j.clon.2007.02.010
- Dahl, E., Kristiansen, G., Gottlob, K., Klamann, I., Ebner, E., Hinemann, B., et al. (2006). Molecular profiling of laser-microdissected matched tumor and normal breast tissue identifies karyopherin alpha2 as a potential novel prognostic marker in breast cancer. *Clin. Cancer Res.* 12 (13), 3950–3960. doi:10.1158/1078-0432.CCR-05-2090
- de Wit, N. J. W., Rijntjes, J., Diepstra, J. H. S., van Kuppevelt, T. H., Weidle, U. H., Ruitter, D. J., et al. (2005). Analysis of differential gene expression in human melanocytic tumour lesions by custom made oligonucleotide arrays. *Br. J. Cancer* 92 (12), 2249–2261. doi:10.1038/sj.bjc.6602612
- Duan, H., Jiang, K., Wei, D., Zhang, L., Cheng, D., Lv, M., et al. (2018). Identification of epigenetically altered genes and potential gene targets in melanoma using bioinformatic methods. *Onco. Targets. Ther.* 11, 9–15. doi:10.2147/OTT.S146663
- El Hassouni, B., Sarkisjan, D., Vos, J. C., Giovannetti, E., and Peters, G. J. (2019). Targeting the ribosome biogenesis key molecule fibrillarin to avoid chemoresistance. *Curr. Med. Chem.* 26 (33), 6020–6032. doi:10.2174/0929867326666181203133332
- Fan, G., Tu, Y., Chen, C., Sun, H., Wan, C., Cai, X., et al. (2018). DNA methylation biomarkers for hepatocellular carcinoma. *Cancer Cell Int.* 18, 140. doi:10.1186/s12935-018-0629-5
- Feng, R., Gong, J., Wu, L., Wang, L., Zhang, B., Liang, G., et al. (2017). MAPK and Hippo signaling pathways crosstalk via the RAF-1/MST-2 interaction in malignant melanoma. *Oncol. Rep.* 38 (2), 1199–1205. doi:10.3892/or.2017.5774
- Flaherty, K. T., Hodi, F. S., and Fisher, D. E. (2012). From genes to drugs: Targeted strategies for melanoma. *Nat. Rev. Cancer* 12 (5), 349–361. doi:10.1038/nrc3218
- Franceschini, A., Szklarczyk, D., Frankild, S., Kuhn, M., Simonovic, M., Roth, A., et al. (2013). STRING v9.1: Protein-protein interaction networks, with increased coverage and integration. *Nucleic Acids Res.* 41 (Database issue), D808–D815. doi:10.1093/nar/gks1094
- Gadeliya Goodson, A., and Grossman, D. (2009). Strategies for early melanoma detection: Approaches to the patient with nevi. *J. Am. Acad. Dermatol.* 60 (5), 719–735. doi:10.1016/j.jaad.2008.10.065
- Gardner Melissa, K., Zanic, M., Gell, C., Bormuth, V., and Howard, J. (2011). Depolymerizing kinesins Kip3 and MCAK shape cellular microtubule architecture by differential control of catastrophe. *Cell* 147 (5), 1092–1103. doi:10.1016/j.cell.2011.10.037
- Goran Micevic, N. T., Marcus, Bosenberg, and Bosenberg, M. (2017). Aberrant DNA methylation in melanoma: Biomarker and therapeutic opportunities. *Clin. Epigenetics* 9, 34. doi:10.1186/s13148-017-0332-8
- Hanahan, D., and Weinberg Robert, A. (2011). Hallmarks of cancer: The next generation. *Cell* 144 (5), 646–674. doi:10.1016/j.cell.2011.02.013
- Huang, D. W., Sherman, B. T., Tan, Q., Collins, J. R., Alvord, W. G., Roayaei, J., et al. (2007). The DAVID gene functional classification tool: A novel biological module-centric algorithm to functionally analyze large gene lists. *Genome Biol.* 8 (9), R183. doi:10.1186/gb-2007-8-9-r183
- Ignacio Blanco, K. K., Cuadras, Daniel, Cuadras, D., Wang, X., Barrowdale, D., de Garibay, G. R., et al. (2015). Assessing associations between the AURKA-HMMR-TPX2-TUBG1 functional module and breast cancer risk in BRCA1:2 mutation carriers. *Plos One* 10, e0120020. doi:10.1371/journal.pone.0120020
- James, G., and Herman, S. B. B. (2003). Gene silencing in cancer in association with promoter hypermethylation. *N. Engl. J. Med. Overseas. Ed.* 349, 2042–2054. doi:10.1056/nejmra023075
- Jonsson, M., Fjeldbo, C. S., Holm, R., Stokke, T., Kristensen, G. B., Lyng, H., et al. (2019). Mitochondrial function of CKS2 oncoprotein links oxidative phosphorylation with cell division in chemoradioresistant cervical cancer. *Neoplasia* 21 (4), 353–362. doi:10.1016/j.neo.2019.01.002
- Kim, J. E., Finlay, G. J., and Baguley, B. C. (2013). The role of the hippo pathway in melanocytes and melanoma. *Front. Oncol.* 3, 123. doi:10.3389/fonc.2013.00123
- Koh, C. M., Gurel, B., Sutcliffe, S., Aryee, M. J., Schultz, D., Iwata, T., et al. (2011). Alterations in nucleolar structure and gene expression programs in prostatic neoplasia are driven by the MYC oncogene. *Am. J. Pathol.* 178 (4), 1824–1834. doi:10.1016/j.ajpath.2010.12.040
- Koynovaa, D. K., Jordanova, E. S., Milev, A. D., Dijkman, R., Kirov, K. S., Toncheva, D. I., et al. (2007). Gene-specific fluorescence *in-situ* hybridization analysis on tissue microarray to refine the region of chromosome 20q amplification in melanoma. *Melanoma Res.* 17, 37–41.
- Lahtz, C., Stranzenbach, R., Fiedler, E., Helmbold, P., and Dammann, R. H. (2010). Methylation of PTEN as a prognostic factor in malignant melanoma of the skin. *J. Invest. Dermatol.* 130 (2), 620–622. doi:10.1038/jid.2009.226
- Laura, T., Smith, J. M., and NormaNowak, J. (1120). 1 amplification in giant-cell tumor of bone: Array CGH, FISH, and association with outcome. *Genes Chromosom. Cancer* 45, 957–966.
- Lawrence, C. J., Dawe, R. K., Christie, K. R., Cleveland, D. W., Dawson, S. C., Endow, S. A., et al. (2004). A standardized kinesin nomenclature. *J. Cell Biol.* 167 (1), 19–22. doi:10.1083/jcb.200408113
- Liang, H. B., Cao, Y., Ma, Q., Shu, Y. J., Wang, Z., Zhang, F., et al. (2017). MYBL2 is a potential prognostic marker that promotes cell proliferation in gallbladder cancer. *Cell. Physiol. Biochem.* 41 (5), 2117–2131. doi:10.1159/000475454
- Livak, K. J., and Schmittgen, T. D. (2001). Analysis of relative gene expression data using real-time quantitative PCR and the 2⁻(Delta Delta C(T)) Method. *Methods* 25 (4), 402–408. doi:10.1006/meth.2001.1262
- Lu, J. J., Chen, F. J., Li, Y., Xu, X., Peng, C., Yu, N., et al. (2022). DTL promotes melanoma progression through rewiring cell glucose metabolism. *Ann. Transl. Med.* 10 (2), 68. doi:10.21037/atm-21-6648
- Lu, Y. C., Yao, X., Crystal, J. S., Li, Y. F., El-Gamil, M., Gross, C., et al. (2014). Efficient identification of mutated cancer antigens recognized by T cells associated with durable tumor regressions. *Clin. Cancer Res.* 20 (13), 3401–3410. doi:10.1158/1078-0432.CCR-14-0433
- Mackintosh, C., Ordonez, J. L., Garcia-Dominguez, D. J., Sevillano, V., Llombart-Bosch, A., Szuhaik, K., et al. (2012). 1q gain and CDT2 overexpression underlie an aggressive and highly proliferative form of Ewing sarcoma. *Oncogene* 31 (10), 1287–1298. doi:10.1038/onc.2011.317
- Marcel, V., Ghayad Sandra, E., Belin, S., Therizols, G., Morel, A-P., Solano-González, E., et al. (2013). p53 acts as a safeguard of translational control by regulating fibrillarin and rRNA methylation in cancer. *Cancer Cell* 24 (3), 318–330. doi:10.1016/j.ccr.2013.08.013

- Mohammadpour, A., Derakhshan, M., Darabi, H., Hedayat, P., and Momeni, M. (2019). Melanoma: Where we are and where we go. *J. Cell. Physiol.* 234 (4), 3307–3320. doi:10.1002/jcp.27286
- Moore, L. D., Le, T., and Fan, G. (2013). DNA methylation and its basic function. *Neuropsychopharmacology* 38 (1), 23–38. doi:10.1038/npp.2012.112
- Mori, T., O'Day, S. J., Umetani, N., Martinez, S. R., Kitago, M., Koyanagi, K., et al. (2005). Predictive utility of circulating methylated DNA in serum of melanoma patients receiving biochemotherapy. *J. Clin. Oncol.* 23 (36), 9351–9358. doi:10.1200/JCO.2005.02.9876
- Newton, K., Petfalski, E., Tollervey, D., and Caceres, J. F. (2003). Fibrillarin is essential for early development and required for accumulation of an intron-encoded small nucleolar RNA in the mouse. *Mol. Cell. Biol.* 23 (23), 8519–8527. doi:10.1128/mcb.23.23.8519-8527.2003
- Pan, H. W., Chou, H. Y., Liu, S. H., Peng, S. Y., Liu, C. L., Hsu, H. C., et al. (2006). Role of L2DTL, cell cycle-regulated nuclear and centrosome protein, in aggressive hepatocellular carcinoma. *Cell Cycle* 5 (22), 2676–2687. doi:10.4161/cc.5.22.3500
- Pan, W-W., Zhou, J-J., Yu, C., Xu, Y., Guo, L-J., Zhang, H-Y., et al. (2013). Ubiquitin E3 ligase crl4cdt2/DCAF2as a potential chemotherapeutic target for ovarian surface epithelial cancer. *J. Biol. Chem.* 288 (41), 29680–29691. doi:10.1074/jbc.M113.495069
- Ping Wei, N. Z., Xu, Ye, Li, Xinxiang, Shi, Debing, Wang, Yuwei, Li, Dawei, et al. (2013). TPX2 is a novel prognostic marker for the growth and metastasis of colon cancer. *J. Transl. Med.* 11, 313. doi:10.1186/1479-5876-11-313
- Ren, J., Du, Y., Li, S., Ma, S., Jiang, Y., Wu, C., et al. (2019). Robust network-based regularization and variable selection for high-dimensional genomic data in cancer prognosis. *Genet. Epidemiol.* 43 (3), 276–291. doi:10.1002/gepi.22194
- Rhodes, D. R., Kalyana-Sundaram, S., Mahavisno, V., Varambally, R., Yu, J., Briggs, B. B., et al. (2007). OncoPrint 3.0: Genes, pathways, and networks in a collection of 18,000 cancer gene expression profiles. *Neoplasia* 9 (2), 166–180. doi:10.1593/neo.07112
- Schadendorf, D., van Akkooi, A. C. J., Berking, C., Griewank, K. G., Gutzmer, R., Hauschild, A., et al. (2018). Melanoma. *Lancet* 392 (10151), 971–984. doi:10.1016/S0140-6736(18)31559-9
- Schinke, C., Mo, Y., Yu, Y., Amiri, K., Sosman, J., Grealley, J., et al. (2010). Aberrant DNA methylation in malignant melanoma. *Melanoma Res.* 20 (4), 253–265. doi:10.1097/CMR.0b013e328338a35a
- Siegel, R. L., Miller, K. D., and Jemal, A. (2020). Cancer statistics, 2020. *Ca. Cancer J. Clin.* 70 (1), 7–30. doi:10.3322/caac.21590
- Smoot, M. E., Ono, K., Ruscheinski, J., Wang, P. L., and Ideker, T. (2011). Cytoscape 2.8: New features for data integration and network visualization. *Bioinformatics* 27 (3), 431–432. doi:10.1093/bioinformatics/btq675
- Su, H., Xu, T., Ganapathy, S., Shadfan, M., Long, M., Huang, T. H., et al. (2014). Elevated snoRNA biogenesis is essential in breast cancer. *Oncogene* 33 (11), 1348–1358. doi:10.1038/ncr.2013.89
- Subramanian, A., Tamayo, P., Mootha, V. K., Mukherjee, S., Ebert, B. L., Gillette, M. A., et al. (2005). Gene set enrichment analysis: A knowledge-based approach for interpreting genome-wide expression profiles. *Proc. Natl. Acad. Sci. U. S. A.* 102 (43), 15545–15550. doi:10.1073/pnas.0506580102
- Tanemura, A., Terando, A. M., Sim, M-S., van Hoesel, A. Q., de Maat, M. F. G., Morton, D. L., et al. (2009). CpG island methylator phenotype predicts progression of malignant melanoma. *Clin. Cancer Res.* 15 (5), 1801–1807. doi:10.1158/1078-0432.CCR-08-1361
- Tang, Z., Li, C., Kang, B., Gao, G., Li, C., Zhang, Z., et al. (2017). Gepia: A web server for cancer and normal gene expression profiling and interactive analyses. *Nucleic Acids Res.* 45 (W1), W98–W102. doi:10.1093/nar/gkx247
- Tseng, S-F., Wu, K-J., and Teng, S. C. (2005). Importin KPNA2 is required for proper nuclear localization and multiple functions of NBS1. *J. Biol. Chem.* 280 (47), 39594–39600. doi:10.1074/jbc.M508425200
- Ueki, T., Nishidate, T., Park, J. H., Lin, M. L., Shimo, A., Hirata, K., et al. (2008). Involvement of elevated expression of multiple cell-cycle regulator, DTL/RAMP (denticleless/RA-regulated nuclear matrix associated protein), in the growth of breast cancer cells. *Oncogene* 27 (43), 5672–5683. doi:10.1038/onc.2008.186
- van der Watt, P. J., Maske, C. P., Hendricks, D. T., Parker, M. I., Denny, L., Govender, D., et al. (2009). The Karyopherin proteins, Crm1 and Karyopherin beta1, are overexpressed in cervical cancer and are critical for cancer cell survival and proliferation. *Int. J. Cancer* 124 (8), 1829–1840. doi:10.1002/ijc.24146
- Vera, O., Bok, I., Jasani, N., Nakamura, K., Xu, X., Mecozzi, N., et al. (2021). A MAPK/miR-29 Axis suppresses melanoma by targeting MAFG and MYBL2. *Cancers (Basel)* 13 (6), 1408. doi:10.3390/cancers13061408
- Wallace, H., Elder, D. E., Guerry, D., Epstein, M. N., Greene, M. H., and Van Horn M. (1984). A study of tumor progression: The precursor lesions of superficial spreading and nodular melanoma. *Hum. Pathol.* 15 (12), 1147–1165. doi:10.1016/s0046-8177(84)80310-x
- Weiyang Cai, X. D., Li, Jingjing, Li, J., and Li, Z. (2018). Methylation analysis highlights novel prognostic criteria in human-metastasized melanoma. *J. Cell. Biochem.* 2019, 11990–12001. doi:10.1002/jcb.28484
- Winnepenninckx, V., Lazar, V., Michiels, S., Dessen, P., Stas, M., Alonso, S. R., et al. (2006). Gene expression profiling of primary cutaneous melanoma and clinical outcome. *J. Natl. Cancer Inst.* 98 (7), 472–482. doi:10.1093/jnci/djj103
- Wouters, J., Vizoso, M., Martinez-Cardus, A., Carmona, F. J., Govaere, O., Laguna, T., et al. (2017). Comprehensive DNA methylation study identifies novel progression-related and prognostic markers for cutaneous melanoma. *BMC Med.* 15 (1), 101. doi:10.1186/s12916-017-0851-3
- Wu, C., Zhang, Q., Jiang, Y., and Ma, S. (2018). Robust network-based analysis of the associations between (epi)genetic measurements. *J. Multivar. Anal.* 168, 119–130. doi:10.1016/j.jmva.2018.06.009
- Yang, F., Li, S., Cheng, Y., Li, J., and Han, X. (2020). Karyopherin α 2 promotes proliferation, migration and invasion through activating NF- κ B/p65 signaling pathways in melanoma cells. *Life Sci.* 252, 117611. doi:10.1016/j.lfs.2020.117611
- Yang, L., Dai, J., Ma, M., Mao, L., Si, L., Cui, C., et al. (2019). Identification of a functional polymorphism within the 3'-untranslated region of denticleless E3 ubiquitin protein ligase homolog associated with survival in acral melanoma. *Eur. J. Cancer* 118, 70–81. doi:10.1016/j.ejca.2019.06.006
- Yao, Y., Zuo, J., and Wei, Y. (2018). Targeting of TRX2 by miR-330-3p in melanoma inhibits proliferation. *Biomed. Pharmacother.* 107, 1020–1029. doi:10.1016/j.biopha.2018.08.058
- Yu, M. H., Luo, Y., Qin, S. L., Wang, Z. S., Mu, Y. F., and Zhong, M. (2015). Up-regulated CKS2 promotes tumor progression and predicts a poor prognosis in human colorectal cancer. *Am. J. Cancer Res.* 5, 2708–2718.
- Zhang, C., Zhang, B., Meng, D., and Ge, C. (2019). Comprehensive analysis of DNA methylation and gene expression profiles in cholangiocarcinoma. *Cancer Cell Int.* 19, 352. doi:10.1186/s12935-019-1080-y